Letters in Applied NanoBioScience
Open-Access Journal (ISSN: 2284-6808)

Article
Volume 13, Issue 4, 2024, 195
https://doi.org/10.33263/LIANBS134.195

Staphylococcus epidermidis (Gram +) and *Escherichia coli* (Gram -) Bacteria Show Sensitivity Against Hymecromone Divalent Transition Metal Complexes of Cobalt and Copper

Tolis Panayi [1,2], Manos C. Vlasiou [3,*]

1. Department of Life, School of Life and Health Sciences, University of Nicosia, 2417, Nicosia, Cyprus
2. Department of Health, School of Life and Health Sciences, University of Nicosia, 2417, Nicosia, Cyprus
3. School of Veterinary Medicine, University of Nicosia, 2414, Nicosia Cyprus

* Correspondence: vlasiou.m@unic.ac.cy;

Scopus Author ID 56019849700

Received: 10.06.2023; Accepted: 12.05.2024; Published: 28.08.2024

Abstract: Antimicrobial resistance is an urgent global public health threat. Pathogenic bacteria, like Escherichia coli and Staphylococcus species, are responsible for zoonotic diseases and high economic loss in farming and the food industry. Our strategy was to create a new chelate ligand derivative from the hymecromone drug and stabilize divalent metal ions to increase the drug's antibacterial activity. Cobalt (II) and Copper (II) complexes showed significant antibacterial activity compared with the established antibiotic Kanamycin. The copper complex had a minimum inhibition concentration of 30 mg/ml, while the cobalt one had a 20 mg/ml MIC.

Keywords: antibacterial; metal; complexes.

1. Introduction

Staphylococcus Epidermidis is one of the most common species found in humans, and it is considered an important opportunistic pathogen. It is also essential in veterinary medicine since tetracycline resistance is high in animals and isolates [1]. On the other hand, *Escherichia coli* is one of the principal inhabitants of most mammalian species' intestinal tract; pathogenic strains can cause diarrhea and hemorrhagic colitis in animals [2]. Nowadays, a significant health emergency is the spread of antimicrobial resistance. This is due to the appearance of resistant strains of the microorganism when an antibiotic molecule is continuously administrated [3]. This situation has increased the incidence of spreading bacteria in farm animals and food-borne diseases. An example of a high-prevalence infectious disease with considerable economic loss worldwide is mastitis in dairy cattle [4, 5]. Various pathogens cause mastitis, mainly *Staphylococcus* species (gram-positive) and *E. coli* (gram-negative) bacteria. These pathogens are categorized as either contagious or environmental, primarily based on the bacterial source and the manner of spread [5]. Another example of high economic loss due to antimicrobial resistance is the spoilage of meat and meat products. These are highly prone to microbial contamination since they are rich in nutrients and other factors, such as fresh meat's pH and water activity [6]. Based on that, there is a high demand worldwide for new antibacterial

substances that can stop the spread of gram-positive and gram-negative bacteria like *Staphylococcus epidermidis* and *Escherichia coli*.

Hymecromone is an approved prescription drug for treating biliary spasms [7]. It belongs to the family of coumarins, most of which are naturally occurring benzopyrene derivatives identified in plants, bacteria, and fungi [8]. Coumarin derivatives have outstanding applications in medicine and biology, and they are available to form coordination compounds with transition metal ions [9, 10]. Their chelating ability increased the biological activity of coumarin derivatives in a way that the properties of the drug are improved when the biomolecules chelate with metal ions. Thus, it helps enhance the compounds' biochemical and catalytic activities [11, 12]. Coordination compounds are also naturally present in the human body for proper growth and maintenance of the body [13]. Transition metals are well-known cations typically used in metal complex formation due to their electrical, magnetic, and catalytic characteristics. Especially transition divalent metal ions like cobalt (Co), copper (Cu), and zinc (Zn) are essential for vital biological functions in humans, and their deficiency can cause disease [14–16].

In this work, we synthesized an imino-di-ethanol derivative of hymecromone coumarin to increase the chelating ability of the molecule to stabilize zinc, cobalt, and copper. After the ligands and complexes were characterized, they were tested for reactivity using quantum calculations. The next step was to perform molecular docking studies on *Staphylococcus* gyrase and *E. coli* DNA gyrase. DNA gyrase is an essential enzyme in bacteria, and its inhibition disrupts DNA synthesis and, subsequently, cell death [17, 18]. Finally, we performed antibacterial essays on *Staphylococcus epidermidis* (Gram +) and *Escherichia Coli* (Gram -) bacteria. Co (II) and Cu (II) metal complexes showed antibacterial activity, with the cobalt complex being more active than the cobalt counter.

2. Materials and Methods

Reagents and solvents were purchased from Merc and used directly without any purification. Ligand and complexes were characterized by ^{1}HNMR and ^{13}CNMR, recorded on Bruker 300 MHz spectrometer using DMSO-d6 as the solvent and TMS as the internal standard. Chemical shifts were expressed in δ ppm. IR measurements were taken on a JASCO (Tokyo, Japan) FT/IR-6600 Spectrometer and an Elemental Vario EL III analyzer was used for the synthesized complexes' elemental analysis. The following species of bacteria were used in the study for the microbiological analysis: *Staphylococcus epidermis* ATCC 12228 and *Escherichia coli* ATCC 25,922. Minimum inhibitory concentrations (MICs) of the complexes against the test organisms were also detected.

2.1. Experimental.

2.1.1. Synthesis of 6-((bis(2-hydroxyethyl)amino)methyl)-7-hydroxy-4-methyl-2H-chromen-2-one (Ligand).

The bis Mannich hymecromone derivative was synthesized by the corresponding 7-hydroxy-4-methyl-2H-chromen-2-one, following the classical conditions of the Mannich reaction for phenolic compounds. In this way, we have incorporated the chelate group of 2,2'-azanediyldiethanol into hymecromone. The solution of 7-hydroxy-4-methyl-2H-chromen-2-one (200 mg, 0.68 mmol), with 0.02 mL of 15% HCl (aq) in 10 mL of MeOH and formaldehyde (0.68 mmol), was stirred at room temperature [19–21]. Secondary amine (2,2'-

azanediyldiethanol) (0.68 mmol) was added dropwise, and the reaction mixture was stirred and refluxed at 80°C for three hours. The solvent was removed under pressure and dried over anhydrous Na_2SO_4. The crude solid was recrystallized with EtOAc to yield the Ligand 89 %. ^{1}H NMR (300 MHz, DMSO-d6): δ 2.42 (s, -CH_3 methyl), 2.53 (m, -CH_2 methylene), 3.45 (s, -CH_2 methylene), 3.65 (s, -OH alcohol), 3.65 (s, -OH alcohol), 5.35 (s, -OH alcohol), 6.23 (s, -H coumarin), 6.81 (s, -OH aromatic), 7.40 (s, -OH aromatic), ppm. IR (KBr, cm^{-1}): ~2880 (m, br, *v*(OH)), 1900 (m, *v*(C=C)), 1630 (m, *v*(C-C)), 1200 (s, *v*(C-N)), 900 (s, *v*(C-H)). Formula: $C_{15}H_{19}NO_5$. Molecular weight: 293.32. m/z: 293.13 (100.0%), 294.13 (16.6%), 295.13 (2.3%).

2.1.2. Synthesis of the divalent metal complexes of Zn, Cu (II), and Co (II).

The three metal complexes of the hymecromone ligand were synthesized using the same procedure. In a round bottom flask of 50 ml, an ethanolic solution of the newly synthesized ligand was refluxed for four h with $CoCl_2$, $ZnCl_2$, and $CuCl_2$ at a 1:1 ratio. The precipitated solids were collected after cooling the flasks in ice. The collected solids were dried under a vacuum. [Co(II) (L) Cl_2], [Cu(II) (L) Cl_2], [Zn(II) (L) Cl_2].

[Co(II) (L) Cl_2]: IR (KBr, cm^{-1}): ~3270 (w, *v*(O-H)), 2040 (s, *v*(C=C)), 1100 (s, *v*(C-C)), 1300 (m, *v*(C-N), 801 (w, *v*(C-H), 580 (s, *v*(M-N)). Formula: $C_{15}H_{17}Cl_2CoNO_5$. Molecular weight: 421.14. Elemental analysis: C: 42.78, H: 4.07, Cl: 16.84, Co: 13.99, N: 3.33, O: 19.00.

[Cu(II) (L) Cl_2]: IR (KBr, cm^{-1}): ~3840 (w, v(O-H)), 2100 (s, v(C=C)), 1810 (s, v(C-C)), 1220 (m, v(C-N), 810 (w, v(C-H), 510 (s, v(M-N)). Formula: $C_{15}H_{17}Cl_2CuNO_5$. Molecular weight: 425.75. Elemental analysis: C: 42.32, H: 4.02, Cl: 16.65, Cu14.93, N: 3.29, O: 18.79.

[Zn(II) (L) Cl_2]: IR (KBr, cm^{-1}): ~3210 (w, v(O-H)), 2050 (s, v(C=C)), 1630 (s, v(C-C)), 1320 (m, v(C-N), 1100 (w, v(C-H), 550 (s, v(M-N)). Formula: $C_{15}H_{17}Cl_2ZnNO_5$. Molecular weight: 427.58. Elemental analysis: C: 42.13, H: 4.01, Cl: 16.58, Zn: 15.29, N: 3.28, O: 18.71.

2.1.3. Antibacterial assay.

Staphylococcus epidermidis ATCC 12228 and *Escherichia coli* ATCC 25922 species were used in the study for the antimicrobial screening. The spot assay method was used. Briefly, a single colony of the desired strain was used to inoculate 15 ml broth media (LB broth from Sigma for *E.coli* or TSB from Fisher Scientific for *S. epidermidis*) and incubated at 37°C overnight. The overnight culture was subsequently diluted 1000-fold into sterilized LB agar or TSB agar that had cooled down to 50°C, mixed, and then poured into sterile 120 mm X 120 mm Petri dishes and allowed to set. Serial two-fold dilutions in DMSO of the tested compounds (the newly synthesized ligand (6-((bis(2-hydroxyethyl)amino)methyl)-7-hydroxy-4-methyl-2H-chromen-2-one) and the divalent metal complexes ([Co(II) (L) Cl_2], [Cu(II) (L) Cl_2], [Zn(II) (L) Cl_2]) were created and spotted unto the petri dish in 50 µl spots. The plates were incubated at 37°C for 24 hours before evaluating the results. The minimum inhibitory concentrations were determined as the dilution where the spot was completely clear and not turbid using Kanamycin 50 mg/ml as a positive control and DMSO as a negative control.

2.2. Theoretical evaluation.

2.2.1. Quantum studies.

The study continued with the quantum-based investigation of the newly synthesized ligand and their corresponding metal complexes (C1-C3). Theoretical calculations included geometry optimizations and computations of the harmonic vibrations followed by TDDFT calculations of the electronic absorption spectrum [22]. The calculations were performed using the B3LYP functional and pcseg-2 basis set using ORCA software [23–25]. The QTAIM (quantum theory of atoms in molecules) analysis and the molecular models and orbitals were performed using the Chem 3D Pro 12.0 program and Chemcraft software.

2.2.2. Molecular docking.

Docking calculations were performed using iGEMDOCK v2.1 [26, 27] software, with the following settings (population size 800, generations 80, and a number of solutions 10), for the complex structures C_1-C_3 over the DNA gyrase of *Staphylococcus* species and *E. coli* [PDB:4URO, 6RKV]. The structures of the complexes were created using the AVOGADRO application version 1.2.0. [28], after structure optimization using ORCA software.

2.2.3. Molecular dynamics.

The protein-ligand complexes were placed in a rectangular parallelepiped water box, and an explicit solvent model for water was used. In contrast, the complexes were solvated with a 10 Å water cap. Chlorine ions were added as counterions to neutralize the system. Before the MD simulations, energy minimization was carried out, and the MD trajectories were run using the minimized structures as starting conformations. The time step of the simulations was 2.0 fs, and a cutoff of 10 Å for the non-bonded interactions. Constant-volume periodic boundary MD was carried out for 300 ps. The temperature was constant at 298 K. All ligands that showed an average RMSD greater than 2 Å concerning the reference disposition were discarded using the docking result as a reference pose [29].

3. Results and Discussion

3.1. Results.

As mentioned above, the novel hymecromone-amino substitute ligand was synthesized based on the Mannich reaction of a secondary amine. In Figure 1, we can see the 2D and 3D structures of the ligand 6-((bis(2-hydroxyethyl)amino)methyl)-7-hydroxy-4-methyl-2H-chromen-2-one. In addition, after reacting the ligand with metal salts of zinc, copper, and cobalt, in a 1:1 ratio, three new metal complexes resulted [Co(II) (L) Cl_2], [Cu(II) (L) Cl_2], [Zn(II) (L) Cl_2], as seen in Figure 1 as well. The ligand and its new metal complexes were characterized physiochemically with ^{1}HNMR, ^{13}CNMR, IR, and elemental analysis. Selected IR frequencies for the ligand and its complexes can be found in Table 1. The complete physicochemical profile of the compounds is in Table 2. Important information was also gathered by the HOMO-LUMO values taken by TDDFT studies. The data relies on the stability and reactivity of the molecules. Figure 2 shows the HOMO-LUMO values and Δgap energies for the ligand (left) and cobalt complex (right). The cobalt complex seems more stable than the

other two (Table 2) since it has the lowest gap energy, whereas the copper complex is the most reactive, having the highest gap energy.

The antibacterial activity was further evaluated in the structural and physicochemical evaluation of the compounds. First, molecular docking studies on selected protein structures will be used, followed by an actual in vitro evaluation of gram-positive and gram-negative bacteria. The *in silico* molecular docking evaluation was performed with the crystal protein structures of DNA gyrase. Figure 3 used the protein data bank's protein structures for the *in-silico* assessment. We have selected two different structures derived from *staphylococcus* and *E. coli* species. More details regarding the amino acid residues and the binding energies of those proteins on the selected compounds can be found in Table 3. The amino acids forming hydrogen bonds are red in the table, and the van der Waals interaction amino acids are purple. Amino acid residue interactions on the copper and cobalt complexes with the PDB:4URO protein crystal structure can be seen in Figure 4. In green are the amino acids forming hydrogen bonds with the complexes, and in red are the amino acids interacting with hydrophobic interactions.

Finally, the *in vitro* evaluation of the compounds against *Staphylococcus epidermidis* (gram-positive) and *Escherichia coli* (gram-negative) pathogenic bacteria reveal that from the compounds tested, [Co(II) (L) Cl_2] and [Cu(II) (L) Cl_2] metal compounds have antibacterial activity. The results of the total antibacterial work can be seen in Table 4.

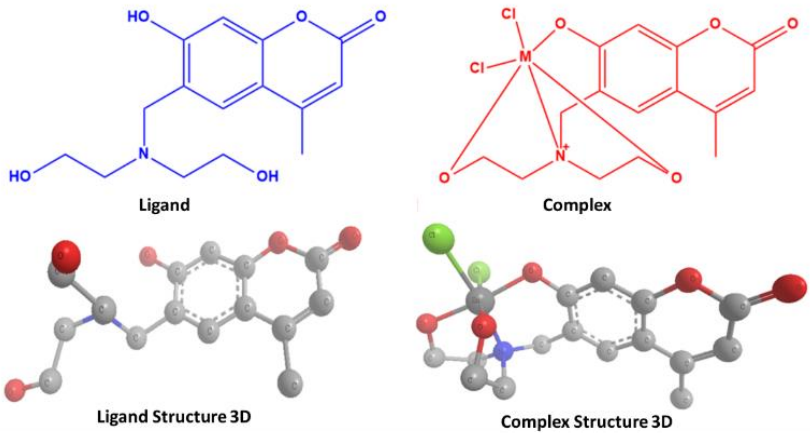

Figure 1. 2D and below 3D structures of the novel hymecromone amino-substitute ligand (left) and its metal complexes (right). (M: is for Co, Cu, or Zn).

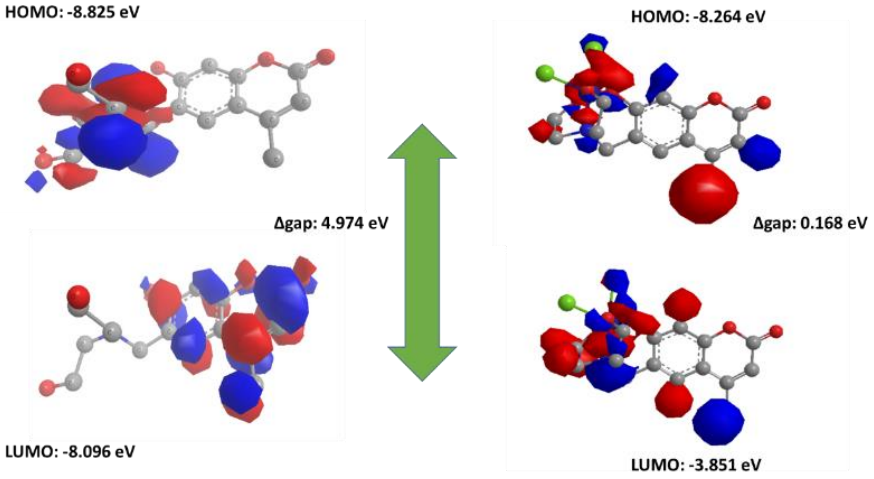

Figure 2. HOMO-LUMO values and *Δ*gap energies for the ligand (left) and cobalt complex (right).

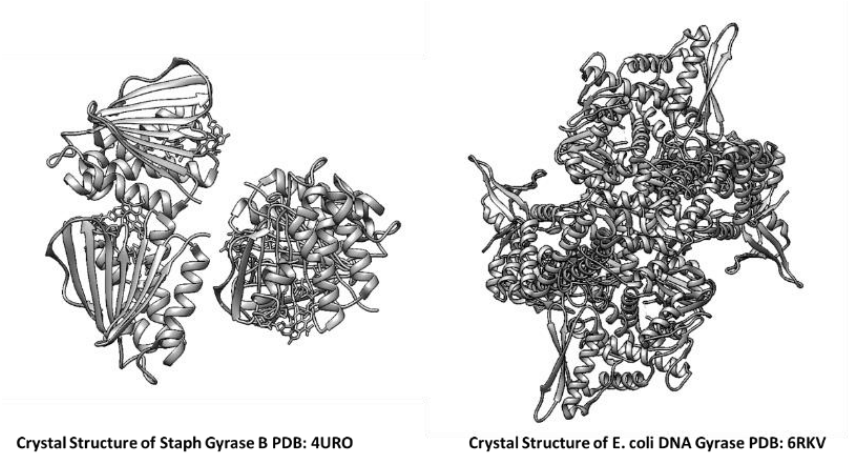

Figure 3. 3D crystal structures as taken by the protein data bank for Staph. and *E. coli* gyrase proteins.

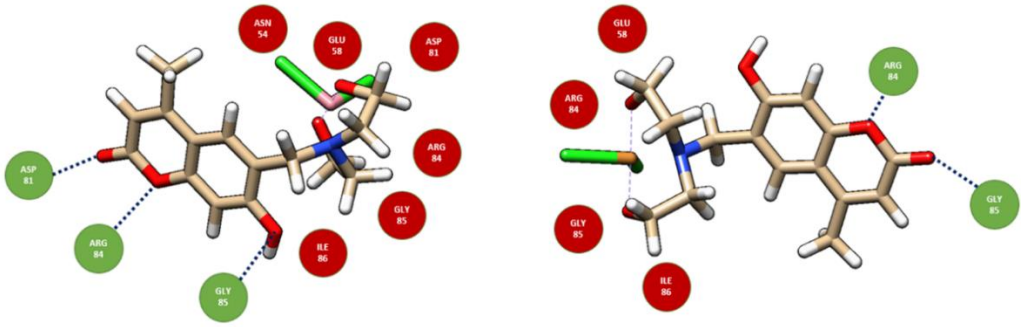

Figure 4. Amino acid residue interactions on the copper (left) and cobalt (right) complexes. The amino acid residues belong to the PDB:4URO protein crystal structure. In green are the amino acids forming hydrogen bonds with the complexes, and in red are the amino acids interacting with hydrophobic interactions.

Table 1. Selected IR frequencies of the ligand and its complexes.

Ligand/Complexes	***v* (OH)**	***v* (C=C)**	***v* (C-C)**	***v* (C-N)**	***v* (C-H)**	***v* (M-N)**
L= (Hymecromone Derivative)	2880	1900	1630	1200	900	---
[Co(II)(L)Cl_2]	3270	2040	1100	1300	801	580
[Cu(II)(L)Cl_2]	3840	2100	1810	1220	810	510
[Zn(II)(L)Cl_2]	3210	2050	1630	1320	1100	550

Table 2. Analytical and physical data of the ligand and its complexes.

Ligand/ Complexes	**Formula (molecular)**	**Molecular weight (g/mol)**	**Elemental analysis (%)**	**HOMO (eV)**	**LUMO (eV)**	**Δgap (eV)**
L= (Hymecromone Derivative)	$C_{15}H_{19}NO_5$	293.32	---	-8.825	-3.851	4.974
[Co(II)(L)Cl_2]	$C_{15}H_{17}Cl_2CoNO_5$	421.14	C:42.78, H:4.07, Cl:16.84, Co:13.99, N:3.28, O:18.71	-8.264	-8.096	0.168
[Cu(II)(L)Cl_2]	$C_{15}H_{17}Cl_2CuNO_5$	425.75	C:42.32, H:4.02, Cl:16.65, Cu:14.93, N:3.33, O:19.00	-11.705	-10.101	1.604
[Zn(II)(L)Cl_2]	$C_{15}H_{17}Cl_2ZnNO_5$	427.58	C:42.13, H:4.01, Cl:16.58, Zn:16.29, N:3.28, O:18.71	-11.707	-10.338	1.369

Table 3. Molecular docking results, energies, and amino acid residues of the study. (In red, the amino acids form hydrogen bonds; in purple, the van der Waals interaction amino acids).

Ligand/Complex Interaction with 4URO PDB	**Binding Energy (KJ/mol)**	**Van der Waals Forces (KJ/mol)**	**Hydrogen Bonds (KJ/mol)**	**Amino Acid Residue**
Ligand	-89.94	-73.28	-16.66	ASP81, ARG84, GLY85, THR173, GLU58, ARG84, GLY85, ILE86
[Co(II)(L)Cl_2]	-95.16	-76.68	-18.48	ARG84, GLY85, GLU58, ARG84, GLY85, ILE86

[Cu(II)(L)Cl_2]	-96.09	-77.53	-18.56	ASP81, ARG84, GLY85, ASN54, GLU58, ASP81, ARG84, GLY85, ILE86
[Zn(II)(L)Cl_2]	-96.06	-75.99	-20.07	ASP81, ARG84, GLY85, THR173, ASN54, GLU58, ASP81, ARG84, GLY85, ILE86
Ligand/Complex Interaction with 6KRV PDB	**Binding Energy (KJ/mol)**	**Van der Waals Forces (KJ/mol)**	**Hydrogen Bonds (KJ/mol)**	**Amino Acid Residue**
Ligand	-87.37	-71.73	-15.64	SER111, ALA117, ASN269, GLN94, PHE96, GLY114, ASP115, SER116, ALA117
[Co(II)(L)Cl_2]	-81.23	-63.26	-17.97	ARG99, MET101, ARG518
[Cu(II)(L)Cl_2]	-81.28	-66.39	-14.89	GLN411, ARG438, ASP194, GLU295
[Zn(II)(L)Cl_2]	-79.70	-59.45	-14.87	HIS80, ALA499, GLY741, TYR149

Table 4. Summary of the MIC values of the tested compounds against *Staphylococcus epidermidis* and *Escherichia coli*.

Ligand/Complex	***Staphylococcus epidermidis* (MIC)**	***Escherichia coli* (MIC)**
Ligand	No activity	No activity
[Co(II)(L)Cl_2]	20 mg/ml	20 mg/ml
[Cu(II)(L)Cl_2]	30 mg/ml	30 mg/ml
[Zn(II)(L)Cl_2]	No activity	No activity

3.2. Discussion.

The main band shift from 2880 cm^{-1} to 3270, 3840, and 3210 cm^{-1} reveals the complexation of the ligand with the cobalt, copper, and zinc metal ions, respectively. Further, the bands at 580, 510, and 550 cm^{-1} were attributed to the metal-nitrogen stretching vibrations [30]. The comparison between the IR spectra of ligands and the metal complexes showed an expressive decrease in the wavelength of C=C stretching vibrations. The formation of the ligand and its complexes were also confirmed by NMR spectroscopy.

Molecular orbitals theory is being employed to describe the chemical behavior of stability, reactivity, and charge transfer [31–33]. From the HOMO-LUMO energy values and chemical reactivity descriptors, we can communicate that the [Co(II)(L)Cl_2] is showing the highest chemical stability, whereas the [Cu(II)(L)Cl_2] has the most increased reactivity amongst the compounds [34, 35]. All the metal complexes have higher reactivity than the ligand. The results are in good agreement with the molecular docking studies since the [Cu(II)(L)Cl_2] has a slightly higher binding energy compared with the [Co(II)(L)Cl_2]. On the other hand, all the metal complexes, including the [Zn(II)(L)Cl_2] one, have higher binding energies than the ligand on the 4URO protein structure (DNA Gyrase of *Staphylococcus*). Additionally, the complexes [Co(II)(L)Cl_2] and [Cu(II)(L)Cl_2] are showing higher binding energies than the [Zn(II)(L)Cl_2], on the 6KRV protein structure (DNA Gyrase of *E. coli*).

More specifically, [Co(II)(L)Cl_2] is connected to the binding pocket of the 4URO with two hydrogen bonds with ARG84 and GLY85, while the hydrophobic interactions of the metal complex with the protein are between the GLU58, ARG84, GLY85, and ILE86 amino acids. The same molecule is bound to the 6RKV protein with hydrogen bonds only between ARG99, MET101, and ARG518 amino acids. Regarding the [Cu(II)(L)Cl_2] complex, is bound with three hydrogen bonds on 4URO protein with ASP81, ARG84, GLY85 and interacting hydrophobically with ASN54, GLU58, ASP81, ARG84, GLY85 and ILE86 amino acids. Regarding the 6KRV protein structure, the same molecule has two hydrogen bonds with GLN411 and ARG438 amino acids and interacts hydrophobically with ASP194 and GLU295 amino acids [9, 36–39]

The studies continued with the *in vitro* evaluation of the ligand and its four complexes on *Staphylococcus epidermidis* (gram-positive) and *E. coli* (gram-negative) bacteria. The study

showed that the amino-substituted hymecromone ligand (6-((bis(2-hydroxyethyl)amino)methyl)-7-hydroxy-4-methyl-2H-chromen-2-one) and the metal complex [Zn(II)(L)Cl_2], didn't show any particular activity against these two strains. On the other hand, the metal complexes of [Co(II)(L)Cl_2] and [Cu(II)(L)Cl_2] showed antibacterial activity compared to the reference antibiotic Kanamycin. In particular, [Co(II)(L)Cl_2] had a MIC value of 20 mg/ml on both strains, while the [Cu(II)(L)Cl_2] had a MIC value of 30 mg/ml on both strains as well. Taking this into consideration, we do believe that these two metal complexes of the hymecromone ligand derivative, [Co(II)(L)Cl_2] and [Cu(II)(L)Cl_2], are worth further investigation in terms of different pathogen bacterial species and *in vivo* evaluation.

4. Conclusions

In this work, we synthesized a novel amino substitute hymecromone derivative and prepared three novel complexes of the divalent metal ions of zinc, copper, and cobalt. After their characterization, these complexes were evaluated *in silico* and *in vitro* for their antibacterial activity, showing promising results. The copper complex had a minimum inhibition concentration of 30 mg/ml, and the cobalt complex had 20 mg/ml MIC. This work opens a new avenue for research against antimicrobial resistance. Established drugs can be complexed with transition metals and evaluated against different pathogenic bacteria.

Funding

None

Acknowledgments

None

Conflicts of Interest

The authors declare no conflict of interest.

References

1. Argudín, M.A.; Vanderhaeghen, W.; Vandendriessche, S.; Vandecandelaere, I.; André, F.-X.; Denis, O.; Coenye, T.; Butaye, P. Antimicrobial resistance and population structure of *Staphylococcus epidermidis* recovered from animals and humans. *Vet. Microbiol.* **2015**, *178*, 105–113, https://doi.org/10.1016/j.vetmic.2015.04.019.
2. Fairbrother, J.M.; Nadeau, É. *Escherichia coli:* on-farm contamination of animals. *Revue Sci. Techn.* **2006**, *25*, 555–569, https://doi.org/10.20506/rst.25.2.1682.
3. Foti, M.; Grasso, R.; Fisichella, V.; Mascetti, A.; Colnaghi, M.; Grasso, M.; Spena, M.T. Antimicrobial Resistance in Physiological and Potentially Pathogenic Bacteria Isolated in Southern Italian Bats. *Animals* **2023**, *13*, 966, https://doi.org/10.3390/ani13060966.
4. Arbab, S.; Ullah, H.; Bano, I.; Li, K.; Ul Hassan, I.; Wang, W.; Qadeer, A.; Zhang, J. Evaluation of in vitro antibacterial effect of essential oil and some herbal plant extract used against mastitis pathogens. *Vet. Med. Sci.* **2022**, *8*, 2655–2661, https://doi.org/10.1002/vms3.959.
5. Ghazy, T.A.; Sayed, G.M.; Farghaly, D.S.; Arafa, M.I.; Abou-El-Nour, B.M.; Sadek, A.M. *In vitro* antiprotozoal effect of alcoholic extract of hemolymph of *Galleria mellonella* larva against *Trichomonas gallinae*. *Int. J. Vet. Sci.* **2023**, *12*, 302–308, https://doi.org/10.47278/journal.ijvs/2022.192.
6. Jayasena, D.D.; Jo, C. Essential oils as potential antimicrobial agents in meat and meat products: A review. *Trends Food Sci. Technol.* **2013**, *34*, 96–108, https://doi.org/10.1016/j.tifs.2013.09.002.

7. Yang, S.; Ling, Y.; Zhao, F.; Li, W.; Song, Z.; Wang, L.; Li, Q.; Liu, M.; Tong, Y.; Chen, L.; Ru, D.; Zhang, T.; Zhou, K.; Zhang, B.; Xu, P.; Yang, Z.; Li, W.; Song, Y.; Xu, J.; Zhu, T.; Shan, F.; Yu, W.; Lu, H. Hymecromone: a clinical prescription hyaluronan inhibitor for efficiently blocking COVID-19 progression. *Sig. Transduct. Target Ther.* **2022**, *7*, 91, https://doi.org/10.1038/s41392-022-00952-w.
8. Kim, G.B.; Hyun, C.-G. The hyaluronan synthesis inhibitor 7-hydroxy-4-methylcoumarin inhibits LPS-induced inflammatory response in RAW 264.7 macrophage cells. *J. Appl. Biol. Chem.* **2021**, *64*, 263–268, https://doi.org/10.3839/jabc.2021.036.
9. Sunitha, N.; Raj, C.I.S.; Kumari, B.S. Synthesis, spectral studies, biological evaluation and molecular docking studies of metal complexes from coumarin derivative. *J. Mol. Struct.* **2023**, *1285*, 135443, https://doi.org/10.1016/j.molstruc.2023.135443.
10. Bouhaoui, A.; Eddahmi, M.; Dib, M.; Khouili, M.; Aires, A.; Catto, M.; Bouissane, L. Synthesis and Biological Properties of Coumarin Derivatives. A Review. *ChemistrySelect* **2021**, *6*, 5848–5870, https://doi.org/10.1002/slct.202101346.
11. Fathalla, S.K.; El-Ghamry, H.A.; Gaber, M. Ru(III) complexes of triazole based Schiff base and azo dye ligands: An insight into the molecular structure and catalytic role in oxidative dimerization of 2-aminophenol. *Inorg. Chem. Commun.* **2021**, *129*, 108616, https://doi.org/10.1016/j.inoche.2021.108616.
12. Kant, R.; Maji, S. Synthesis, characterization and biological evaluation of piperazine embedded copper complexes. *Inorganica Chim. Acta* **2023**, *552*, 121515, https://doi.org/10.1016/j.ica.2023.121515.
13. Retnam, C.T.G.; Rose, S.V.; Kumari, B.S. Synthesis, characterization, biological activity and molecular docking study of transition metal complexes from heterocyclic ligand system. *J. Mol. Struct.* **2023**, *1282*, 135162, https://doi.org/10.1016/j.molstruc.2023.135162.
14. Dawar, N.; Devi, J.; Kumar, B.; Dubey, A. Synthesis, Characterization, Pharmacological Screening, Molecular Docking, DFT, MESP, ADMET Studies of Transition Metal(II) Chelates of Bidentate Schiff Base Ligand. *Inorg. Chem. Commun.* **2023**, *151*, 110567, https://doi.org/10.1016/j.inoche.2023.110567.
15. Govindarajan, K.; Perumalswamy sekar, P.; Ramasamy, K.; Ezhumalai, D.; Rajasekhar Kavitha, R.; Parasuraman, V. Biological screening of divalent transition metal decanoates owning powerful antimicrobial and cytotoxic properties. *J. Drug Deliv. Sci. Technol.* **2023**, *84*, 104428, https://doi.org/10.1016/j.jddst.2023.104428.
16. Abdel-Rahman, L.H.; Abdelghani, A.A.; AlObaid, A.A.; El-ezz, D.A.; Warad, I.; Shehata, M.R.; Abdalla, E.M. Novel Bromo and methoxy substituted Schiff base complexes of Mn(II), Fe(III), and Cr(III) for anticancer, antimicrobial, docking, and ADMET studies. *Sci. Rep.* **2023**, *13*, 3199, https://doi.org/10.1038/s41598-023-29386-2.
17. Elsamra, R.M.I.; Masoud, M.S.; Ramadan, A.M. Designing metal chelates of halogenated sulfonamide Schiff bases as potent nonplatinum anticancer drugs using spectroscopic, molecular docking and biological studies. *Sci. Rep.* **2022**, *12*, 20192, https://doi.org/10.1038/s41598-022-24512-y.
18. Eakin Ann, E.; Green, O.; Hales, N.; Walkup Grant, K.; Bist, S.; Singh, A.; Mullen, G.; Bryant, J.; Embrey, K.; Gao, N.; Breeze, A.; Timms, D.; Andrews, B.; Uria-Nickelsen, M.; Demeritt, J.; Loch James, T.; Hull, K.; Blodgett, A.; Illingworth Ruth, N.; Prince, B.; Boriack-Sjodin, P.A.; Hauck, S.; MacPherson Lawrence, J.; Ni, H.; Sherer, B. Pyrrolamide DNA Gyrase Inhibitors: Fragment-Based Nuclear Magnetic Resonance Screening To Identify Antibacterial Agents. *Antimicrob. Agents Chemother.* **2012**, *56*, 1240–1246, https://doi.org/10.1128/AAC.05485-11.
19. Hadjiadamou, I.; Vlasiou, M.; Spanou, S.; Simos, Y.; Papanastasiou, G.; Kontargiris, E.; Dhima, I.; Ragos, V.; Karkabounas, S.; Drouza, C.; Keramidas, A.D. Synthesis of vitamin E and aliphatic lipid vanadium(IV) and (V) complexes, and their cytotoxic properties. *J. Inorg. Biochem.* **2020**, *208*, 111074, https://doi.org/10.1016/j.jinorgbio.2020.111074.
20. Ioannou, K.; Eleftheriou, C.; Drouza, C.; Pafiti, K.S.; Panayi, T.; Keramidas, A.D.; Zacharia, L.C.; Vlasiou, M.C. Novel Zinc and Vanadium (V) Hydroquinonate Complexes: Synthesis and Biological Solution Evaluation. *J. Mol. Struct.* **2022**, *1257*, 132582, https://doi.org/10.1016/j.molstruc.2022.132582.
21. Vlasiou, M.C.; Ioannou, K.; Eleftheriou, C.; Pafiti, K.S.; Zacharia, L.C.; El-Shazly, M. Synthesis and biological evaluation of a new chalconate Co (II/III) complex with cytotoxic activity. *J. Mol. Struct.* **2022**, *1249*, 131567, https://doi.org/10.1016/j.molstruc.2021.131567.
22. Hassan, H.H.A.M.; ELhusseiny, A.F. A new antimicrobial PVC-based polymeric material incorporating bisacylthiourea complexes. *BMC Chem.* **2023**, *17*, 44, https://doi.org/10.1186/s13065-023-00958-7.
23. Neese, F. Software update: the ORCA program system, version 4.0. *Wiley Interdiscip. Rev.: Comput. Mol. Sci.* **2018**, *8*, e1327, https://doi.org/10.1002/wcms.1327.

24. Neese, F. The ORCA program system. *Wiley Interdiscip. Rev. Comput. Mol. Sci.* **2012**, *2*, 73–78, https://doi.org/10.1002/wcms.81.
25. Neese, F.; Wennmohs, F.; Becker, U.; Riplinger, C. The ORCA quantum chemistry program package. *J. Chem. Phys.* **2020**, *152*, 224108, https://doi.org/10.1063/5.0004608.
26. Yang, J.-M.; Chen, C.-C. GEMDOCK: A generic evolutionary method for molecular docking. *Proteins: Struct., Funct., Genet.* **2004**, *55*, 288–304, https://doi.org/10.1002/prot.20035.
27. Yang, J.M. Development and evaluation of a generic evolutionary method for protein–ligand docking. *J. Comput. Chem.* **2004**, *25*, 843–857, https://doi.org/10.1002/jcc.20013.
28. Hanwell, M.D.; Curtis, D.E.; Lonie, D.C.; Vandermeerschd, T.; Zurek, E.; Hutchison, G.R. Avogadro: an advanced semantic chemical editor, visualization, and analysis platform. *J. Cheminform.* **2012**, *4*, 17, https://doi.org/10.1186/1758-2946-4-17.
29. El Moudaka, T.; Murugan, P.; Rahman, M.B.A.; Tejo, B.A. Discovery of *Mycobacterium tuberculosis* CYP121 New Inhibitor via Structure-based Drug Repurposing. *Pertanika J. Sci. Technol.* **2023**, *31*, https://doi.org/10.47836/pjst.31.3.21.
30. Halevas, E.; Matsia, S.; Hatzidimitriou, A.; Geromichalou, E.; Papadopoulos, T.A.; Katsipis, G.; Pantazaki, A.; Litsardakis, G.; Salifoglou, A. A unique ternary Ce(III)-quercetin-phenanthroline assembly with antioxidant and anti-inflammatory properties. *J. Inorg. Biochem.* **2022**, *235*, 111947, https://doi.org/10.1016/j.jinorgbio.2022.111947.
31. Alorini, T.; Daoud, I.; Al-Hakimi, A.N.; Alminderej, F.; Albadri, A.E.A.E. An experimental and theoretical investigation of antimicrobial and anticancer properties of some new Schiff base complexes. *Res. Chem. Intermed.* **2022**, *49*, 1701–1730, https://doi.org/10.1007/s11164-022-04922-3.
32. Goldmeier, M.N.; Khononov, A.; Belakhov, V.; Pieńko, T.; Orbach, N.; Gilad Barzilay, Y.; Baasov, T. Dynamic Intramolecular Cap for Preserving Metallodrug Integrity─A Case of Catalytic Fluoroquinolones. *J. Med. Chem.* **2022**, *65*, 14049–14065, https://doi.org/10.1021/acs.jmedchem.2c01302.
33. Hafsa; Shah, H.U.R.; Ahmad, K.; Ashfaq, M.; Oku, H. Free radical scavenging, antibacterial potentials and spectroscopic characterizations of benzoyl thiourea derivatives and their metal complexes. *J. Mol. Struct.* **2023**, *1272*, 134162, https://doi.org/10.1016/j.molstruc.2022.134162.
34. Adeniyi, A.A.; Ajibade, P.A. Inhibitory activities and possible anticancer targets of Ru(II)-based complexes using computational docking method. *J. Mol. Graph. Model.* **2012**, *38*, 60–69, https://doi.org/10.1016/j.jmgm.2012.08.004.
35. Burgart, Y.; Shchegolkov, E.; Shchur, I.; Kopchuk, D.; Gerasimova, N.; Borisevich, S.; Evstigneeva, N.; Zyryanov, G.; Savchuk, M.; Ulitko, M.; Zilberberg, N.; Kungurov, N.; Saloutin, V.; Charushin, V.; Chupakhin, O. Promising Antifungal and Antibacterial Agents Based on 5-Aryl-2,2′-bipyridines and Their Heteroligand Salicylate Metal Complexes: Synthesis, Bioevaluation, Molecular Docking. *ChemMedChem* **2022**, *17*, e202100577, https://doi.org/10.1002/cmdc.202100577.
36. Sakthikumar, K.; Krause, R.W.M.; Isamura, B.K.; Raja, J.D.; Athimoolam, S. Spectro-electrochemical, fluorometric and biothermodynamic evaluation of pharmacologically active morpholine scaffold single crystal ligand and its metal(II) complexes: A comparative study on *in-vitro* and *in-silico* screening towards DNA/BSA/SARS-CoV-19. *J. Inorg. Biochem.* **2022**, *236*, 111953, https://doi.org/10.1016/j.jinorgbio.2022.111953.
37. Mariswamy, V.H.; Bindya, S.; Costa, R.A.; Prasad, S.K.; Shivamallu, C.; Begum, S.M.; Veerapur, R.; Syed, A.; Kollur, S.P. 2-Methoxy-5-(6-methoxypyridin-3-yl-imino-methyl)phenol and its transition metal complexes as potent antibacterial agents: Synthesis, characterization, theoretical investigations and biological evaluation. *Results Chem.* **2021**, *3*, 100120, https://doi.org/10.1016/j.rechem.2021.100120.
38. Ranjitha, N.; Krishnamurthy, G.; Bhojya Naik, H.S.; Pari, M.; Afroz, L.; Sumadevi, K.R.; Manjunatha, M.N. Structural elucidation, voltammetric detection of dopamine, molecular docking and biological inspection of novel 4-aminoantipyrine derived Schiff bases in Co (II), Ni (II) and Cu (II) complexes. *Inorganica Chim. Acta* **2022**, *543*, 121191, https://doi.org/10.1016/j.ica.2022.121191.
39. Buvaylo, E.A.; Nesterova, O.V.; Goreshnik, E.A.; Vyshniakova, H.V.; Petrusenko, S.R.; Nesterov, D.S. Supramolecular Diversity, Theoretical Investigation and Antibacterial Activity of Cu, Co and Cd Complexes Based on the Tridentate N,N,O-Schiff Base Ligand Formed In Situ. *Molecules* **2022**, *27*, 8233, https://doi.org/10.3390/molecules27238233.